Supplementary Information (SI)

Dilute lattice doping of ^{64}Cu into 2D-nanoplate; its impact on radio-labeling efficiency and stability for target selective PET imaging

Sairan Eom, [a,b] *Min Hwan Kim,* [b] *Ranji Yoo,* [b] *Goeun Choi,*[c,d,e] *Joo Hyun Kang,* [b] *Yong Jin Lee,* [b] *and Jin-Ho Choy**[c,f,g]

[a]Center for Intelligent Nano-Bio Materials (CINBM), Department of Chemistry and Nanoscience, Ewha Womans University, Seoul 03760, Republic of Korea

[b]Division of Applied-RI, Korea Institute of Radiological and Medical Sciences, Seoul 01812, Republic of Korea

[c]Intelligent Nanohybrid Materials Laboratory (INML), Institute of Tissue Regeneration Engineering (ITREN), Dankook University, Cheonan 31116, Republic of Korea

[d]College of Science and Technology, Dankook University, Cheonan 31116, Republic of Korea.

[e]Department of Nanobiomedical Science and BK21 PLUS NBM Global Research Center for Regenerative Medicine, Dankook University, Cheonan 31116, Republic of Korea.

[f]Department of Pre-medical Course, College of Medicine, Dankook University, Cheonan 31116, Republic of Korea

[g]Tokyo Tech World Research Hub Initiative (WRHI), Institute of Innovative Research, Tokyo Institute of Technology, Yokohama 226-8503, Japan

*Corresponding author. E-mail: jhchoy@dankook.ac.kr

S1. Materials and Methods

S1. 1 Synthesis of the ^{64}Cu radioisotope physically adsorbed on QT-NPs, ^{64}Cu-ads-QT-NPs and the BSA coated, ^{64}Cu-ads-QT-NPs/BSA as the control groups.

In order to compare the radiolabeling efficiency and stability of ^{64}Cu isomorphically doped into QT-NPs with those of ^{64}Cu physically adsorbed on external surface of QT-NPs, the two control samples, ^{64}Cu-ads-QT-NPs and ^{64}Cu-ads-QT-NPs/BSA were prepared as follows [1]; QT-NPs were synthesized by hydrothermal method at 100 °C for 12 h, and thus prepared suspension (15 mg/mL) was added into 0.1M sodium acetate solution (pH = 5.5) containing ~ 185 MBq of ^{64}Cu radioisotopes. And then the mixed solution was treated under a constant shaking condition at 37 °C for 3 h.

S1. 2 *In-vitro* cytotoxicity study of ^{64}Cu-QT-NPs and ^{64}Cu-QT-NPs/BSA

The human breast cancer cell line (MDA-MB-231) was purchased from the American Type Culture Collection (ATCC) and cultured in the Roswell Park Memorial Institute (RPMI) 1640 medium (WelGENE, Republic of Korea) with 10 % fetal bovine serum (FBS) and 1 % antibiotics (both by Invitrogen, USA) under an atmosphere of 5 % CO_2 and 95 % air at 37 °C. To investigate cell viability based on trypan blue exclusion assay, the MDA-MB-231 cells were seeded onto 24-well plates (5×10^4 cells/well), incubated at 37 °C for ~12 h under a 5% CO_2 atmosphere, and finally exposed to the samples Cu-QT-NPs, and Cu-QT-NPs/BSA, respectively, in the concentration range of 1–100 μg/mL and further incubated for 48h. After incubation at the progress time, the cells were washed twice with phosphate-buffered saline (PBS), and detached with 0.1 % trypsin. The detached cells were collected in the media, and 20 μL of cell suspension was diluted with 20 μL of 0.4 % trypan

blue. Finally, viable cells were counted within the grids on hemacytometer, and their cell viability (%) was calculated as the following equation;

$$Cell\ viability\ (\%) = \frac{Total\ number\ of\ viable\ cells}{Total\ number\ of\ cells} \times 100$$

S1. 3 *In-vivo* toxicology study of Cu-QT-NPs

Cu-QT-NPs (10 mg/kg) and saline (100 µl) were intravenously injected to the normal BALB/c mice. The liver and spleen of mice were harvested at 1 week after injection, and then the tissues were stained with H&E (Hematoxylin and Eosin) to confirm histopathology.

S2. Additional data

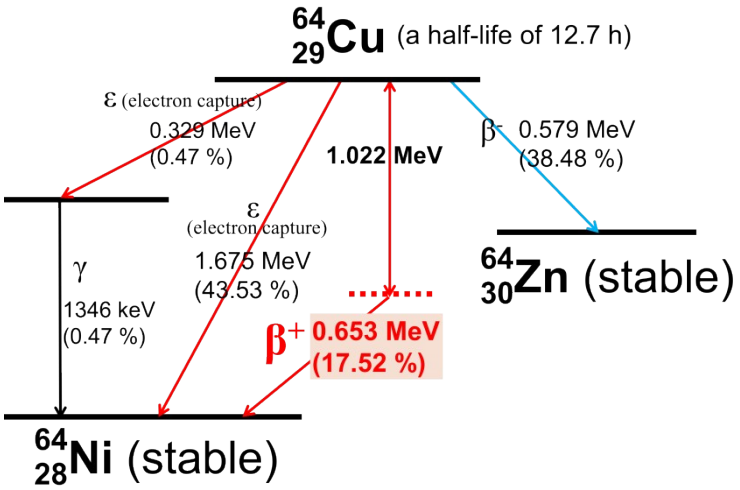

Fig. S1 Decay scheme of ^{64}Cu radioisotope [2].

The ^{64}Cu radioisotope can be produced from proton irradiation on ^{64}Ni target in a medical cyclotron using ^{64}Ni(p, n)^{64}Cu reaction [3]. ^{64}Cu radioisotope with a half-life of 12.7 h is quite useful for PET imaging and for radiotherapeutic applications due to its decay mode of β^+ (18 %), β^- (38.5 %), and electron capture (ε, 43.5 %) of as illustrated in Fig. S1.

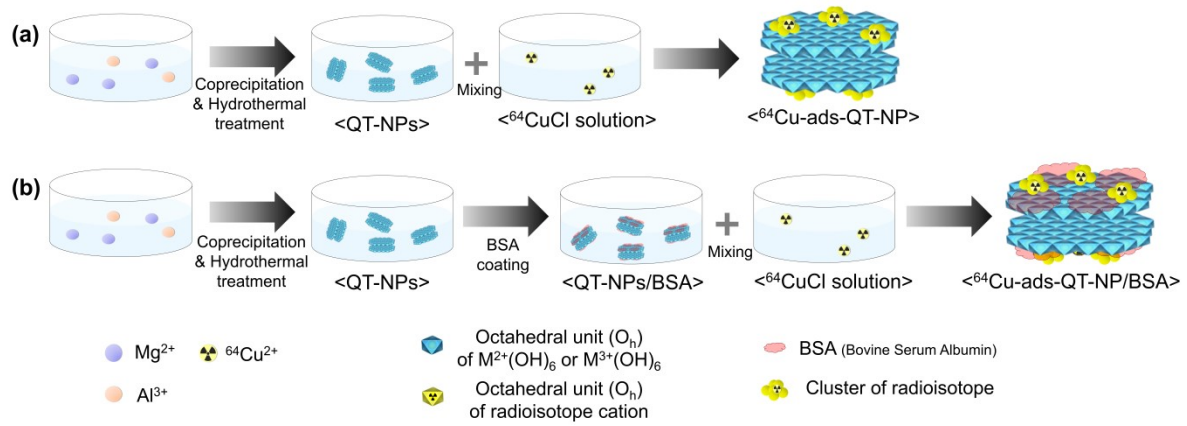

Fig. S2 Structural schemes for the physisorbed ^{64}Cu on external surface of QT-NP (a) ^{64}Cu-ads-QT-NP, and its BSA coated (b) ^{64}Cu-ads-QT-NP/BSA.

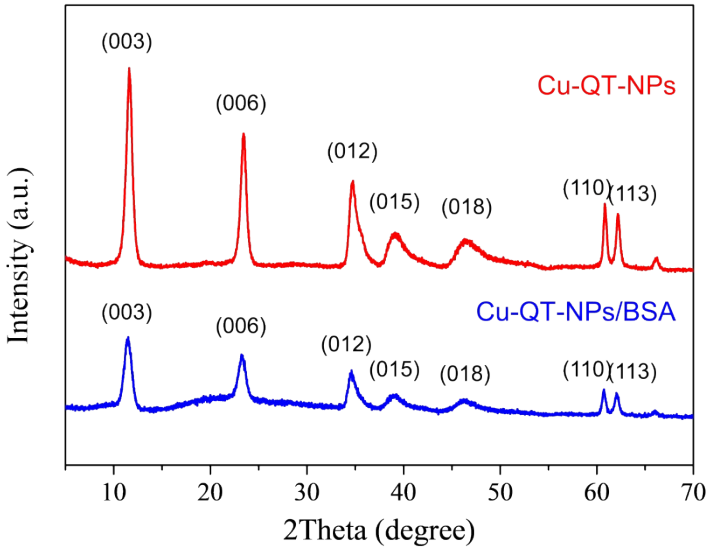

Fig. S3 Powder XRD patterns for Cu-QT-NPs and Cu-QT-NPs/BSA.

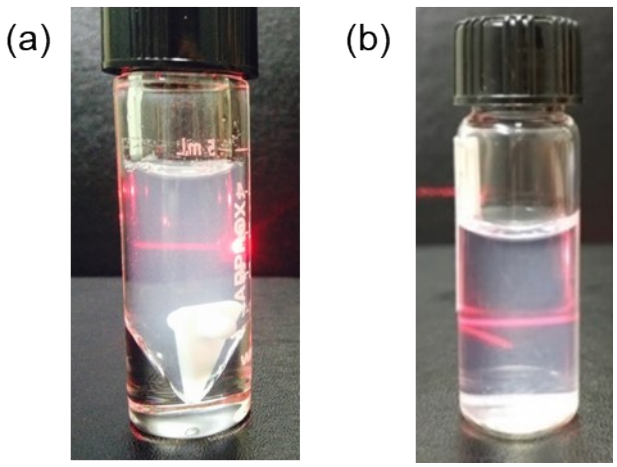

Fig. S4 Colloidal (a) Cu-QT-NPs and (b) Cu-QT-NPs/BSA images.

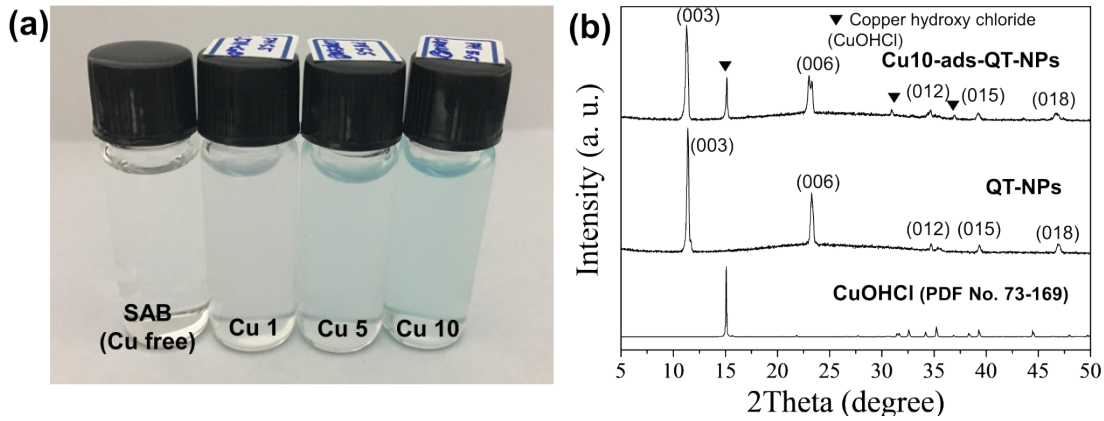

Fig. S5 (a) Images for sodium acetate buffer (SAB) (pH = 5.5) and mixture solution of QT-NPs suspension and SAB containing different concentration of $Cu(II)Cl_2$ (Cu1, Cu5, Cu10). (b) Powder XRD patterns of copper chloride hydroxide (CuOHCl) as an undesired (impurity) phase formed on QT-NPs in Cu10 solution.

The ^{64}Cu radioisotope physically adsorbed on QT-NPs, ^{64}Cu-ads-QT-NPs, showed the low chemical stability (63.4 ± 0.99 %) as expected, due to the fact that the ^{64}Cu phase was weakly bound on the external surface of QT-NPs. But it has not been well understood so far what kind of ^{64}Cu phase was formed on the surface of QT-NPs, and why its labeling stability was so poor [1]. This is surely due to the difficulty in characterizing such an unknown ^{64}Cu surface phase with doping amount on QT-NPs. And therefore, its chemical and structural information were not available as yet, since the doped phase cannot be detected by XRD analyzer due to its detection limit of < 5%. In order to define the unknown surface phase, we attempted to prepare the non-labeled QT-NPs (Cu-ads-QT-NPs) under the same synthetic condition where excess $CuCl_2$ was given as presented in Fig. S5.

At first, QT-NPs were synthesized under a hydrothermal condition of 100 °C and 12 h, and thus prepared suspension was added into the sodium acetate buffer (SAB, 0.1 M) solution (pH = 5.5) with different concentrations of $CuCl_2$ solution (0.1 M). And the mixed solution was kept at 37 °C for 3 h under stirring condition. As shown in Fig. S4(a), Cu1, Cu5 and Cu10 represented the mixed SAB solution containing $CuCl_2$, corresponding to the Cu(II)/Mg(II) molar ratio of 0.01, 0.05, and 0.10, respectively. Since the detection limit of XRD analyzer is < 5 %, no significant impurity was observed in the XRD pattern for QT-NPs with the molar ratio of 0.01 and 0.05. On the other hand, the impurity peak corresponding to the copper hydroxychloride (CuOHCl, PDF No. 73-169) could be detected for QT-NPs with the molar ratio of 0.10, indicating that the Cu(II) ions were physically adsorbed on the external surface of QT-NPs, as the form of CuOHCl. It is, therefore, concluded that the unknown phase containing ^{64}Cu radioisotope physically adsorbed on the surface of QT-NPs was neither copper oxide (CuO) nor copper hydroxide ($Cu(OH)_2$), but CuOHCl (Fig. S2(a) and Fig. S5(b)).

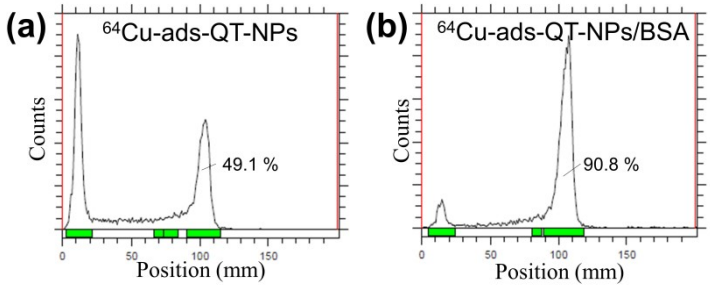

Fig. S6 The radio-TLC graphs of (a) ^{64}Cu-ads-QT-NPs and (b) ^{64}Cu-ads-QT-NPs/BSA.

The labeling efficiency of ^{64}Cu-ads-QT-NPs and ^{64}Cu-ads-QT-NPs/BSA were investigated by radio-TLC using a 20 mM sodium citrate/50 mM EDTA solution (pH = 5.5) as a mobile phase. According to the radio-TLC results (Fig. S6), ^{64}Cu radioisotopes physically adsorbed on QT-NPs were easily released from ^{64}Cu-ads-QT-NPs and ^{64}Cu-ads-QT-NPs/BSA by the mobile phase, because the labeling efficiency for the former was determined to be 50.9 % indicating that the detached ^{64}Cu phase reached to 49.1 % due to its weak bonding with the external surface of QT-NPs as shown in Fig. S6(a). In the latter case, the labeling efficiency became extremely lower down to 9.2 % upon BSA coating; 90.8 % of ^{64}Cu radioisotopes were detached from ^{64}Cu-ads-QT-NPs/BSA. Different from the present isomorphically substituted phases, such low labeling efficiencies of the physically adsorbed ones, ^{64}Cu-ads-QT-NPs and ^{64}Cu-ads-QT-NPs/BSA, could be explained by the fact that ^{64}Cu radioisotopes were formed on external surface of QT-NPs as unknown amorphous phases, such as CuO and $Cu(OH)_2$, including nano-crystalline CuOHCl as clearly demonstrated in the present study. According to the literature [4], CuOHCl is highly soluble at low pH (2.2), and expected to be

136 partly dissolved in the mobile phase with pH = 5.5. The labeling stability, therefore, cannot
137 be expected from the adsorbed phases by simple mixing QT-NPs with ^{64}Cu radioisotope.

139

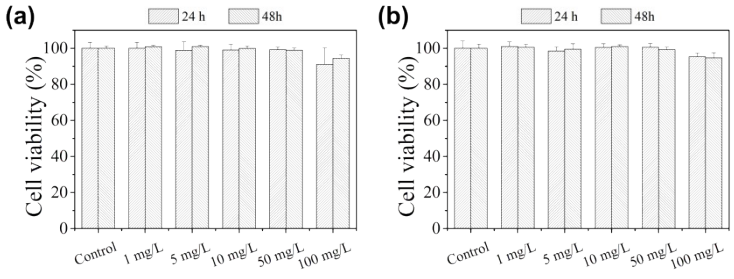

140

141 **Fig. S7** *In-vitro* cytotoxicity of (a) Cu-QT-NPs and (b) Cu-QT-NPs/BSA on the human breast

142 cancer cell line (MDA-MB-231) for 24 and 48 h.

143

144

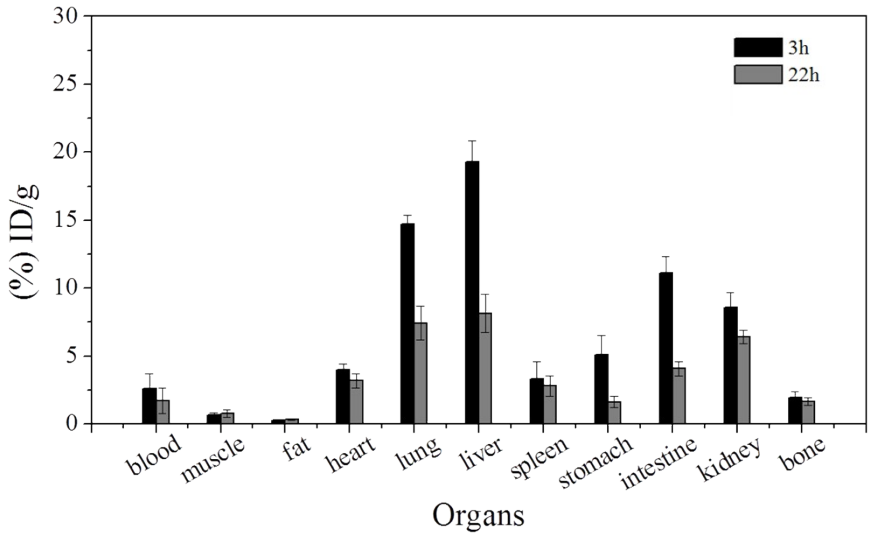

Fig. S8 *In-vivo* biodistribution of ^{64}Cu for 3 and 22 h after *i.v.* injection. It was performed on BALB/c normal mouse model (n = 3), and the %ID/g for each organ was calculated using equation (3).

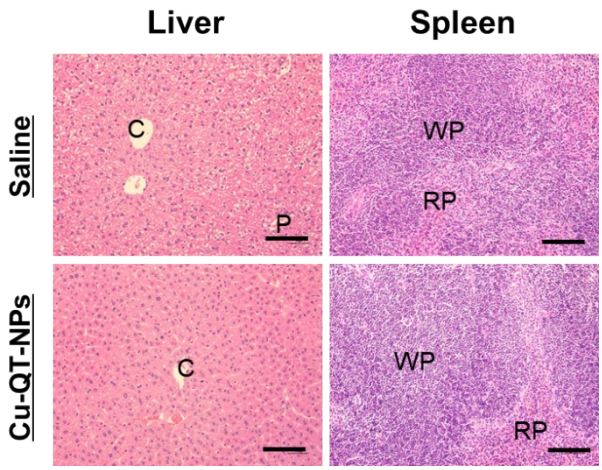

Fig. S9 *In-vivo* toxicology; H&E staining of liver and spleen of mice at 1 week after injection with saline and Cu-QT-NPs. (Scale bar: 100 μm), (C: central vein, P: portal vein, RP: red pulp, WP: white pulp)

Table S1 Labeling efficiencies and stabilities of various ^{64}Cu-labeled nanomaterials

Complexes	Labeling radioactivity (or spatial activity)	Labeling efficiency	Labeling stability	Ref.
^{64}Cu-NOTA[1)]-inhibitor	3-4 mCi (78-246 mCi/μmol)	65-70 %		[5]
^{64}Cu-PCTA[2)]-inhibitor	3-4 mCi (78-246 mCi/μmol)	70-90 %		[5]
^{64}Cu-Oxo-DO3A[3)]-inhibitor	3-4 mCi (78-246 mCi/μmol)	75-85 %		[5]
^{64}Cu-CB-TE2A[4)]-inhibitor	3-4 mCi (78-246 mCi/μmol)	30-45 %		[5]
^{64}Cu-DOTA[5)]-inhibitor	3-4 mCi (78-246 mCi/μmol)	65-70 %		[5]
^{64}Cu-NOTA-BBN[6)]	-	> 90 %		[6]
^{64}Cu-NOTA-FHT[7)]	2 mCi (270-810 μCi/nmol)	> 95 %		[7]
^{64}Cu-DOTA-FA[8)]-dendrimer	1-3 mCi (34 μCi/nmol)	>85 %	93.9 % (20 h)	[8]
^{64}Cu-DOTA-mAb7	1 mCi (6 μCi/μg)	71.9 %	90.6 (24 h) 88.7 (48 h)	[9]
^{64}Cu-NODAGA[9)]-mAb7	1 mCi (5 μCi/μg)	59.3 %	93.4 (24 h) 84.5 (48 h)	[9]
^{64}Cu-TETA-OC[10)]	(~ 1500 mCi/μg)	> 95 %		[10]
^{64}Cu-DOTA-rituximab	1 mCi	98.9 %	54 % (24 h), 26 % (48 h)	[11]
^{64}Cu-DTPA[11)]-rituximab	1 mCi	74.5 %	14 % (48 h)	[11]
^{64}Cu-DOTA-SPIO[12)]	3 mCi (54-108 mCi/mmol)	94 %	97.5 % (24 h)	[12]
^{64}Cu-DOTA-Au	5.76 mCi	81.3 %		[13]
^{64}Cu-NOTA-Au	1 mCi (20 mCi/nmol)	60-70 %		[14]

* 1 mCi = 3.7 x 10^7 Bq

1) NOTA: 1,4,7-triazacyclononane-N,N',N''-triacetic acid

2) PCTA: 3,6,9,15-tetraazabicyclo[9.3.1]-pentadeca-1(15),11,13-triene)-3,6,9-triacetic acid

3) Oxo-DO3A: oxa4,7,1-tetraazacyclododecane-4,7,10-triacetic acid

4) CB-TE2A: 1,4,8,11-tetraazabicyclo[6.6.2]hexadecane-4,11-diacetic acid

5) DOTA: 1,4,7,10-tetraazacyclodoadecane-N,N′,N″,N‴-tetraacetic acid

6) BBN: bombesin

7) FHT: dodecapeptide (Phe-His-Thr-Pro-Ser-Gln-Asn-Ser-Ala-Phe-Arg-Leu)

8) FA: Folic acid

9) NODAGA: 1,4,7-triazacyclononane,1-glutaric acid,4,7-acetic acid

10) TETA-OC: 1,4,8,11-tetraazacyclotetradecane-N,N',N'',N'''-tetraacetic acid- $_{D}$-Phe^{1}-octreotide

11) DTPA: diethylene triamine penta acetic acid

12) SPIO: superparamagnetic iron oxide

Table S2 Time-dependent radioactivities for tumors, muscles, liver, and blood after *i.v.* injection of ^{64}Cu-QT-NPs and ^{64}Cu-QT-BSA-NPs. All the data are represented with the mean ± standard deviation (n = 3)

Sample	Time	Organ (%ID/g)			
		Tumor	Muscle	Liver	Blood
^{64}Cu-QT-NPs	2 h	0.71 ± 0.10	0.63 ± 0.12	29.4 ± 13.47	0.55 ± 0.03
	6 h	1.40 ± 0.29	0.65 ± 0.12	28.6 ± 11.00	0.56 ± 0.03
	24 h	2.13 ± 0.25	0.57 ± 0.06	25.6 ± 10.54	0.55 ± 0.10
	48 h	2.43 ± 0.60	0.53 ± 0.16	23.1 ± 10.27	0.45 ± 0.02
^{64}Cu-QT-NPs/BSA	2 h	0.96 ± 0.36	0.60 ± 0.07	38.6 ± 5.34	0.70 ± 0.10
	6 h	1.80 ± 0.20	0.76 ± 0.14	35.0 ± 6.36	0.93 ± 0.18
	24 h	4.53 ± 0.51	1.35 ± 0.10	29.0 ± 5.73	1.25 ± 0.10
	48 h	4.93 ± 0.81	1.60 ± 0.32	22.9 ± 2.52	1.23 ± 0.19

Table S3 Size distribution of Cu-QT-NPs and Cu-QT-NPs/BSA in saline.

Samples	Particle size
Cu-QT-NPs	585 nm ± 102 * (0.669)
Cu-QT-NPs/BSA	186 nm ± 38 * (0.356)

* PDI: Polydispersity index is shown in parentheses

Table S4 Liver toxicity results for QT nanoparticles from our previous *in-vivo* studies.

Particles	Analysis	Toxicity	Ref.
QT	ALT[1)] and AST[2)] level	No significant difference within normal range (ALT: 7-227 (U/L), AST: 37-329 (U/L))	[15]
MTX-QT	ALT and AST level	No significant difference within normal range (ALT: 7-227 (U/L), AST: 37-329 (U/L))	[15]
QT	Concentration of Mg, Al in liver	No significant difference with control	[15]
MTX-QT	Concentration of MTX in liver	No significant difference with control	[15]
MTX-QT	Concentration of MTX in liver	No significant difference with control	[16]

1) ALT: alanine aminotransferase, 2) AST: aspartate aminotransferase

References

[1] S. Shi, B. C. Fliss, Z. Gu, Y. Zhu, H. Hong, H. F. Valdovinos, R. Hernandez, S. Goel, H. Luo, F. Chen, T. E. Barnhart, R. J. Nickles and Z. P. Xu, *Sci. Rep.*, 2015, **5**, 16930.

[2] "Decay Scheme of ^{64}Cu radioisotope.", Retrieved 16 November 2020. https://www.nucleonica.com/wiki/index.php?title=Decay_Schemes

[3] J. Y. Kim, H. Park, J. C. Lee, K. M. Kim, K. C. Lee, H. J. Ha, T. H. Choi, G. I. An and G. J. Choen, *Appl. Radiat. Isot.*, 2009, **67**, 1190–1194.

[4] E. Caldera, B. Weigel, V. N. Kucharczyk, K. S. Sellins, S. L. Archibeque, J. J. Wagner, H. Han, W. S. Jerry and T. E. Engle, *J. Anim. Sci.*, 2019, **97**, 1852–1864.

[5] S. R. Banerjee, M. Pullambhatla, C. A. Foss, S. Nimmagadda, R. Ferdani, C. J. Anderson, R. C. Mease and M. G. Pomper, *J. Med. Chem.*, 2014, **57**, 2657–2669.

[6] A. F. Prasanphanich, P. K. Nanda, T. L. Rold, L. Ma, M. R. Lewis, J. C. Garrison, T. J. Hoffman, G. L. Sieckman, S. D. Figueroa and C. J. Smith, *Proc. Natl. Acad. Sci.*, 2007, **104**, 12462–12467.

[7] J. R. Merrill, K. Krajewski, H. Yuan, J. E. Frank, D. S. Lalush, C. Patterson and A. N. Veleva, *Biomaterials*, 2016, **84**, 241–249.

[8] W. Ma, F. Fu, J. Zhu, R. Huang, Y. Zhu, Z. Liu, J. Wang, P. S. Conti, X. Shi and K. Chen, *Nanoscale*, 2018, **10**, 6113–6124.

[9] S. C. Ghosh, K. L. Pinkston, H. Robinson, B. R. Harvey, N. Wilganowski, K. Gore, E. M. Sevick-Muraca and A. Azhdarinia, *Nucl. Med. Biol.*, 2015, **42**, 177–183.

[10]L. A. Bass, M. Wang, M. J. Welch and C. J. Anderson, *Bioconju. Chem.*, 2000, **11**, 527–532.

[11]M. S. Cooper, M. T. Ma, K. Sunassee, K. P. Shaw, J. D. Williams, R. L. Paul, P. S. Donnelly and P. J. Blower, *Bioconju. Chem.*, 2012, **23**, 1029–1039.

[12]C. Glaus, R. Rossin, M. J. Welch and G. Bao, *Bioconju. Chem.*, 2010, **21**, 715–722.

[13]H. Xie, B. Goins, A. Bao, Z. J. Wang and W. T. Phillips, *Int. J. Nanomed.*, 2012, **7**, 2227–2238.

[14]K. Cheng, S. R. Kothapalli, H. Liu, A. L. Koh, J. V. Jokerst, H. Jiang, M. Yang, J. Li, J. Levi, J. C. Wu, S. S. Gambhir and Z. Cheng, *J. Am. Chem. Soc.*, 2014, **136**, 3560–3571.

[15]G. Choi, H. Piao, Z. A. Alothman, A. Vinu, C. O. Yun and J. H. Choy, *Int. J. Nanomed.*, 2016, **11**, 337–348.

[16]G. Choi, O. Y. Kwon, Oh, C. O. Yun and J. H. Choy, *Sci. Rep.*, 2014, **4**, 1–7.